ORIGINAL ARTICLE

Population Pharmacokinetics of Morphine in Patients With Nonalcoholic Steatohepatitis (NASH) and Healthy Adults

V Pierre[1], CK Johnston[1,2], BC Ferslew[1], KLR Brouwer[1] and D Gonzalez[1]*

Altered expression and function of transporters in nonalcoholic steatohepatitis (NASH) patients may affect the pharmacokinetics (PK), efficacy, and safety of substrate drugs. A population pharmacokinetic (PopPK) analysis was performed to assess differences in morphine and morphine-3-glucuronide (M3G) disposition in NASH and healthy subjects. A total of 315 serum and 42 urine samples from 21 subjects (14 healthy; 7 NASH) were analyzed using NONMEM. Morphine and M3G PK were described by three- and one-compartment models, respectively. After accounting for the effect of total body weight on all clearance and volume of distribution parameters using an allometric scaling approach, NASH severity score (NASF; combination of fibrosis and nonalcoholic fatty liver disease activity scores) was the most significant predictor of differences in M3G exposure. The model predicted a linear decrease in the clearance of M3G with increasing NASF scores on a natural logarithmic scale. These results may provide some insight into the potential effect of NASH on the disposition of hepatic transporter substrates.
CPT Pharmacometrics Syst. Pharmacol. (2017) **6**, 331–339; doi:10.1002/psp4.12185; published online 18 April 2017.

Study Highlights

WHAT IS THE CURRENT KNOWLEDGE ON THE TOPIC?
☑ The effect of changes in the expression and function of basolateral and apical efflux transporters in patients with nonalcoholic steatohepatitis (NASH) on the disposition of substrate drugs has not been well characterized.
WHAT QUESTION DID THIS STUDY ADDRESS?
☑ A population PK model was developed to assess the impact of NASH status and other plausible covariates on altered morphine and morphine-3-glucuronide (M3G) disposition.
WHAT THIS STUDY ADDS TO OUR KNOWLEDGE
☑ After accounting for the effects of total body weight, this study established a quantitative relationship between NASH severity score, and the exposure of M3G. Increased M3G serum exposure may be due to reduced biliary excretion and increased basolateral efflux of M3G. The results of this study highlight the need for further investigation on the effects of NASH on therapeutic agents with similar hepatic mechanisms of disposition as morphine and its glucuronides.
HOW MIGHT THIS CHANGE DRUG DISCOVERY, DEVELOPMENT, AND/OR THERAPEUTICS?
☑ This model may serve as a framework to guide clinical studies exploring variability in disposition of therapeutic agents that are substrates of hepatic transporters in patients with NASH.

Nonalcoholic fatty liver disease (NAFLD) is a leading cause of chronic liver dysfunction, which affects one-third of the adult population worldwide and up to 70% of patients with type 2 diabetes and obesity.[1–3] Approximately 20% of patients with NAFLD progress to nonalcoholic steatohepatitis (NASH).[4] NASH is a progressive stage of NAFLD that is characterized by hepatic accumulation of triglycerides, inflammation, and hepatocyte injury/degeneration. Insulin resistance, obesity, and metabolic syndrome are comorbidities that are frequently present in patients with NASH.[5] As the disease progresses, these patients are predisposed to developing cirrhosis and subsequently hepatocellular carcinoma.[5] With the increasing prevalence of obesity and diabetes, NASH is predicted to become the leading cause of liver transplantation in the next 15 years.[2]

Liver disease such as NASH can alter the pharmacokinetics (PK) of drugs frequently prescribed in this population.[6] Although the mechanisms for these changes are currently being investigated, alterations in drug transporters and/or drug metabolizing enzymes are likely to play an important role.[7,8] For example, in NASH patients downregulation of the organic anion-transporting polypeptide 1B3 (OATP1B3), which is important for the uptake of some drugs (e.g., statins) into hepatocytes, has been reported.[9,10] Examination of liver tissue from NASH patients revealed a significant decrease in hepatic uptake transporter expression, while the opposite effect was observed for efflux transporters, such as multidrug resistance-associated protein (MRP)2, MRP3, and MRP4.[9] Despite general upregulation of MRP2 protein in the hepatocyte, biliary excretion of Mrp2 substrates was reduced in

[1]Division of Pharmacotherapy and Experimental Therapeutics, UNC Eshelman School of Pharmacy, University of North Carolina at Chapel Hill, Chapel Hill, North Carolina, USA; [2]Metrum Research Group LLC, Tariffville, Connecticut, USA. *Correspondence: D Gonzalez (daniel.gonzalez@unc.edu)

Population PK of Morphine in NASH and Healthy Subjects
Pierre *et al*.

332

rodents with NASH due to the internalization of protein away from the canalicular membrane.[11,12] Recently, an experiment conducted in rodent NASH models has shown a significant increase in the protein expression of the renal efflux transporters Mrp2 and Mrp4.[13] In addition, alterations in the mRNA expression and/or enzymatic activity of several isoforms of cytochrome P450 (CYPs), as well as some phase II enzymes, including glutathione S-transferases (GSTs), sulfotransferases (SULTs), and UDP-glucuronosyltransferases (UGTs), have been observed in human liver tissue collected from NASH patients.[14–16] Remarkably, the consequences of these changes on *in vivo* PK in patients with NASH remains largely unstudied.

Morphine is a commonly used opiate analgesic that exhibits high interindividual variability (IIV) in disposition and response.[17,18] Morphine primarily undergoes glucuronidation to morphine-3-glucuronide (M3G) and morphine-6-glucuronide (M6G) via UGT2B7.[19] Both glucuronides are substrates of hepatic MRP2 and MRP3.[13] Of note, one investigation concluded that there were no statistically significant differences in the mRNA expression of UGT2B7 between liver samples from NASH patients (fatty and non-fatty), patients with steatosis, and normal subjects.[15] Thus, our group performed a clinical study using intravenously administered morphine as a probe substrate to investigate whether altered hepatic basolateral efflux clearance is an important contributor to altered PK in NASH subjects.[21] The results of this study indicated that while morphine exposure did not vary between healthy and NASH subjects, the disposition of the glucuronide metabolites was significantly altered (e.g., increased systemic concentrations of M3G and M6G), likely due to increased hepatic MRP3 and reduced MRP2 function in patients with NASH.[21] The aim of the present study was to use a population PK (PopPK) analysis approach to characterize the variability in the disposition of morphine and its glucuronide metabolites in patients with NASH and healthy subjects.

METHODS
Study design and patient population
Serum and urine concentrations for morphine and glucuronide metabolites were obtained from a previously published study designed to assess the effect of NASH on altered drug disposition.[21] Details of the study design, inclusion and exclusion criteria, and bioanalytical methods for morphine and morphine glucuronide metabolites as well as serum bile acids were described previously.[21,22] Briefly, a single intravenous dose of 5 mg morphine sulfate was infused over 5 min to all study subjects 2 hr after administration of a standardized meal containing 23.9 g of fat that was consumed over 30 min. Primary and secondary bile acid species were measured before and over the 2-hr postmeal period. Specifically, samples were collected at time 0, which corresponded to preprandial concentrations, and 30, 60, 90, and 120 min postprandial. Fourteen healthy (seven females; seven males) and seven subjects with biopsy-confirmed NASH (four females; three males) with a median (range) age of 45 years (20–63) were enrolled. Six out of the 14 healthy subjects had a total body weight <70 kg,

Table 1 Demographic and clinical characteristics of NASH and healthy subjects

Characteristics[a,b]	Healthy (*N* = 14)	NASH (*N* = 7)
Age (years)	43 (20-62)	46 (33-63)
Total body weight (kg)	74 (52-101)	90.3 (77-128)
Body mass index (kg/m^2)	25 (21-29)	30.5 (27-41)
Alkaline phosphatase (U/L)	64 (45-84)	77 (61-98)
Fibroscan score (kPa)	4 (2-6)	13 (5-29)
Creatinine clearance (mL/min)[c]	118 (70-174)	141 (96-188)
Male (%)	7 (50%)	4 (57%)

[a]Data are expressed as median (range).
[b]Previously published by Ferslew *et al*. 2015.[21]
[c]Estimated using the Cockroft-Gault equation.

whereas all of those with NASH were >70 kg (**Table 1**). Serial serum PK samples were collected at the following timepoints: predose, 5, 10, 15, 30, 45, 60, 90, 120, 180, 240, 300, 360, 420, and 480 min after the end of the morphine infusion. Over the 8-hr PK sampling schedule following morphine administration, two urine samples were collected per subject by pooling urine produced over 4-hr intervals. The lower limits of quantification (LLOQ) of the bioanalytical assay for morphine and M3G in serum were 8.24 and 5.42 nanomoles/L (nM), while for urine samples they were 82.4 and 542 nM, respectively. The study was approved by the University of North Carolina at Chapel Hill Biomedical Institutional Review Board.

Population PK analysis
A PopPK analysis was performed using the software NONMEM (v. 7.3, ICON Development Solutions, Ellicott City, MD). R Studio (v. 0.98.1028), the R package ggplot2, Pirana, and Perl-speaks-NONMEM were used for PopPK model development, data visualization, and run management.[23–25] Model development was performed through evaluation of standard goodness-of-fit plots, changes in the objective function value (OFV) and Akaike Information Criterion (AIC), condition number, as well as the precision and plausibility of parameter estimates. The following model diagnostic plots were generated: individual and population predictions vs. observations; conditional weighted residuals (CWRES) vs. time after dose and population predictions; normalized prediction distribution errors (NPDE) vs. time after dose; quantile–quantile plots of NPDEs; and numerical and visual predictive checks (NPC, VPC).[26,27] Nominal observation times were used as bins to calculate summary statistics for the VPC and NPDE plots. A total of 1,500 simulated datasets were generated for the VPC without uncertainty.

The morphine dose in milligrams was converted to nanomoles of morphine free base to facilitate the simultaneous modeling of the parent and metabolite in serum and urine. Prior to analysis, the units of morphine and glucuronide concentrations were converted from ng/mL to nM using each respective molecular weight and then concentrations were subsequently transformed to a natural logarithmic scale. The M3 method was used to fit the concentrations that were below the limit of quantification (BLQ) and reduce bias in model predictions; however, we also compared this

approach to results obtained by ignoring the BLQ data or using a value equal to the lower limit of quantification divided by two.[28] Although measurements for M6G were available, 42% of samples (132/315) were BLQ. Since changes in M3G disposition in the presence of NASH would be expected to reflect changes in M6G, the latter was not included in the PopPK model development as the M6G data did not provide additional value to the primary objective of the study.

Structural model development. A linear mammillary compartmental model was developed using a system of ordinary differential equations implemented through the ADVAN13 subroutine, which solves both stiff and nonstiff systems. The iterative two-stage procedure followed by Monte Carlo importance sampling with Laplacian methods and η-ε interaction were used for parameter estimation and evaluation of the log-likelihood function. Two- and three-compartment structural models with central and peripheral formation clearance of M3G were investigated for morphine, while one- and two-compartment models were assessed for the characterization of the M3G PK data.[29] During model development, these candidate structural models were tested using both macro- and micro-constant parameterization. Initially, IIV parameters were estimated for all morphine and M3G PK terms using an exponential model. IIV parameters were retained in the model based on η-shrinkage, model stability, and successful convergence of the model's covariance step. To assess the residual variability of the log-transformed concentrations, exponential and combined additive and exponential residual error models were assessed.[30] Separate residual error parameters were included for each analyte (morphine and M3G) and sample matrix (serum and urine).

Covariate analysis. Due to pronounced differences in body size between healthy and NASH subjects, total body weight was included *a priori* in the base model as a covariate for all morphine and M3G clearance (CL) and volume of distribution (V) parameters using a power exponent of 0.75 and 1, respectively. Specifically, the CL and V terms were estimated according to the following relationship:

$$CL_i\left(\frac{L}{hr}\right) = CL_{70kg} * \left(\frac{weight_i}{70\ kg}\right)^{0.75} * \exp\left(\eta_{ij}\right) \qquad (1)$$

$$V_i(L) = V_{70kg} * \left(\frac{weight_i}{70\ kg}\right) * \exp\left(\eta_{ij}\right) \qquad (2)$$

Where CL_i and V_i are the estimates of CL and V in the *i*th individual; CL_{70kg} and V_{70kg} represent the clearance and volume of distribution values for a typical 70 kg subject; $weight_i$ represents each subject's total body weight; and η_{ij} is a random variable with mean equal to zero and variance ω^2 that denotes the deviation from the group value (subjects with the same weight) for parameter *j* in the *i*th individual.

A forward inclusion-backward elimination approach was used to assess the significance of additional covariates in explaining the variability in the PK parameters for morphine and M3G. *P*-values of 0.05 (reduction of 3.84 points in the OFV) and 0.01 (reduction of 6.64 points) were used for the forward inclusion and backward elimination steps, respectively.

The following covariates were tested for significance on all parameters where IIV was estimated: NASH status, NASH severity score (NASF), maximum total serum bile acid concentration ($C_{max,BA}$), area under the total serum bile acid concentration vs. time curve from 0 to 120 min ($AUC_{0-120,BA}$), and serum alkaline phosphatase values. NASH status is a binary variable that takes on the value of unity for patients with the condition. NASF is a noninvasive scoring system (ranging from 0 to 12) that combines the NAFLD activity score (NAS) and fibrosis staging to evaluate patients with NASH.[31,32] The NAS score assigns an ordinal measure to the degree of steatosis (0–3 points), hepatocyte ballooning (0–2 points), and lobular inflammation (0–3 points). The fibrosis staging score ranges from 0 to 4 points, depending on the degree of fibrosis from biopsy: a score of 0 reflects the absence of fibrotic tissue; 1, perisinusoidal or pericellular fibrosis; 2, periportal fibrosis; 3, bridging fibrosis; and 4, cirrhosis. Healthy subjects in our study were assigned a NASF score of 0.[21,31,32] Based on prior literature indicating altered bile acid homeostasis in NASH subjects, bile acid exposure measures ($C_{max,BA}$ and $AUC_{0-120,BA}$) were tested as continuous covariates that may explain altered disposition in NASH subjects.[33] Total serum bile acid concentrations were calculated by summing the molar concentration of both conjugated and unconjugated forms of primary and secondary bile acid species.

Continuous and categorical covariates (with the exception of NASF) were described mathematically using power and linear functions, respectively (Eqs. 3 and 4):

$$\theta_{ij} = \theta_{pop,j} * \left(\frac{cov_i}{cov_{median}}\right)\theta_{cov} \qquad (3)$$

$$\theta_{ij} = \theta_{pop,j} * \left(\theta_{cov}\right)^D \qquad (4)$$

Where θ_{ij} and $\theta_{pop,j}$ represent individual and population parameter estimates (for parameter *j* in the *i*th subject), respectively; θ_{cov} represents the effect of disease status on the population estimate of the parameter; cov_i and cov_{median} represent the individual and median values for the covariate; and *D* represents disease status with binary values of 1 and 0 for NASH and healthy subjects, respectively. With the exception of total body weight, continuous covariates were log-transformed prior to analysis. NASF scores specifically were evaluated using a linear model for scores 4 and above (Eq. 5). For NASF scores lower than 4, θ_{cov} was equal to zero. At a NASF score of 4, this covariate effect canceled out (as Ln(1) = 0). The NASF cutoff used to distinguish healthy vs. NASH subjects was based on previous data suggesting that subjects with a score less than 5 are considered to have a benign form of the disease.[31,34]

$$\theta_{ij} = \theta_{pop,j} * \left(1 + \theta_{cov} * Ln\left(\frac{NASF_i}{4}\right)\right) \qquad (5)$$

Simulations. The final model was used to simulate morphine and M3G exposure, without uncertainty, following
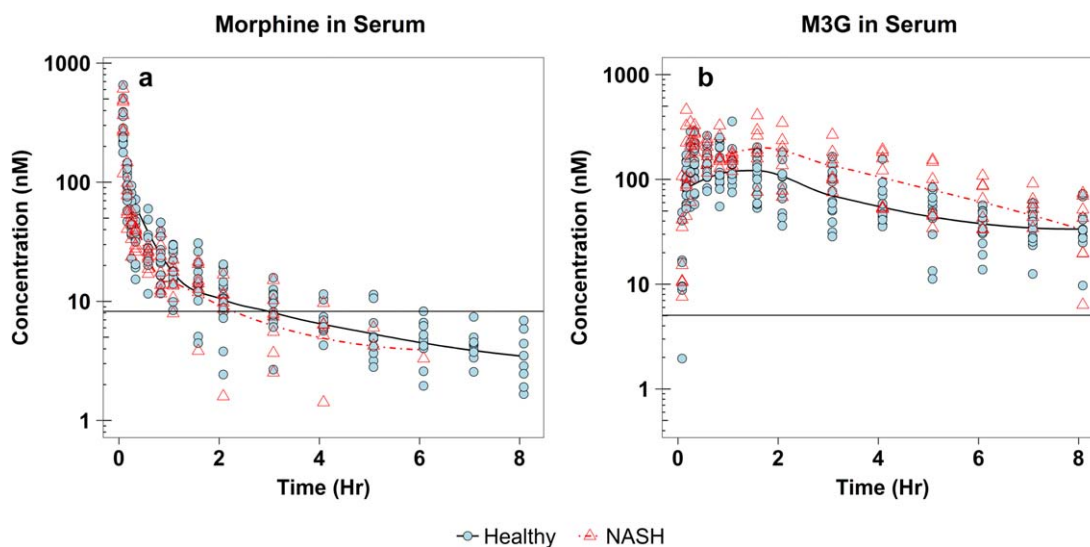
Figure 1 Semilogarithmic concentration vs. time plots of (**a**) morphine and (**b**) morphine-3-glucuronide (M3G) in serum. Data for non-alcoholic steatohepatitis (NASH) and healthy subjects are presented as red triangles and light blue circles, respectively. Least squares lines were overlaid on the serum concentration-time data for NASH and healthy subjects as represented by the dotted red and solid black lines, respectively. The horizontal black lines represent the lower limit of quantification for morphine and M3G.

administration of a 10 mg morphine dose administered intravenously (10-min infusion) every 4 hr for 24 hr. A complete variance-covariance matrix was used to conduct the simulations in order to maintain the correlation between the PK parameters, thus limiting the occurrence of discordant and incongruent PK profiles. The simulation dataset contained 1,000 virtual subjects, half of which had NASH. The distribution of total body weight for healthy and NASH virtual subjects was similar to that in the present study. Since there was no observed trend between weight and NASF severity score, the NASF scores observed in the present study (4, 5, 7, and 8) were randomly assigned to virtual NASH subjects. Also, consistent with the observed data, a NASF severity score of 0 was assigned to all the virtual healthy subjects.

Steady-state area under the concentration vs. time curve from zero to tau was estimated for morphine ($AUC_{M,SS,0-\tau}$) and M3G ($AUC_{M3G,SS,0-\tau}$) using the log-linear trapezoidal method in the ncappc R package.[35] The cumulative amount excreted in urine over 4 hr for both analytes (morphine and M3G) following a single dose also was computed for virtual NASH and healthy subjects. Morphine's clearance (CL_M) was derived as the sum of renal ($CL_{M,R}$) and nonrenal ($CL_{M,NR}$) morphine clearance terms in the model (**Supplementary Figure S1**). A Wilcoxon signed rank test was used to assess differences in simulated steady-state exposure and cumulative amount excreted in urine between the virtual NASH and healthy subjects.

RESULTS
Study population
Fourteen healthy and seven NASH subjects contributed 315 serum and 42 urine samples. For morphine and M3G, 71 (23%) and 1 (<1%) samples, respectively, were BLQ. The median (range) number of quantifiable serum samples

per subject for morphine and M3G were 21 (9–21) and 21 (20–21), respectively. Four (19%) NASH subjects had a body mass index (BMI) >30 kg/m^2 (**Table 1**). All healthy subjects were assigned an NASF severity score of 0. For NASH subjects, one subject each had a score of 4 and 8, whereas two and three subjects had a score of 5 and 7, respectively.

Population PK analysis
Concentration vs. time curves for morphine and M3G are shown in **Figure 4.** A three-compartment model with an additional transit compartment for metabolite conversion described the morphine and M3G data well (**Figure 2**). A one-compartment model was used for M3G (**Supplementary Figure S1**). $CL_{M,NR}$ was assumed to lead exclusively to the formation of M3G. Due to the high residual variability in the M3G urine data, attempts to obtain estimates for additional morphine clearance pathways beyond $CL_{M,NR}$ and $CL_{M,R}$ led to implausible values. These attempts resulted in alternative clearance routes that account for less than 1% of the total morphine systemic clearance compared to the literature reported $\geq$20%.[36] Thus, the fraction metabolized to M3G was assumed to be unity.

After accounting for total body weight differences using an allometric relationship in the base model, only the NASF score reached statistical significance for inclusion in the final model. The off-diagonal correlation between CL_{M3G} and V_{M3G} was estimated at 0.75. Using a linear relationship, the effect of the NASF scores on the apparent clearance of M3G (CL_{M3G}) led to an 8-point reduction in the OFV. The clearance of M3G was inversely correlated to changes in NASF scores on a natural logarithmic scale. On average, individual CL_{M3G} estimates were 6.9, 5.2, and 3.7 L/hr for NASH subjects with NASF scores of 5, 7, and 8, respectively, compared to 8.3 L/hr for healthy subjects.
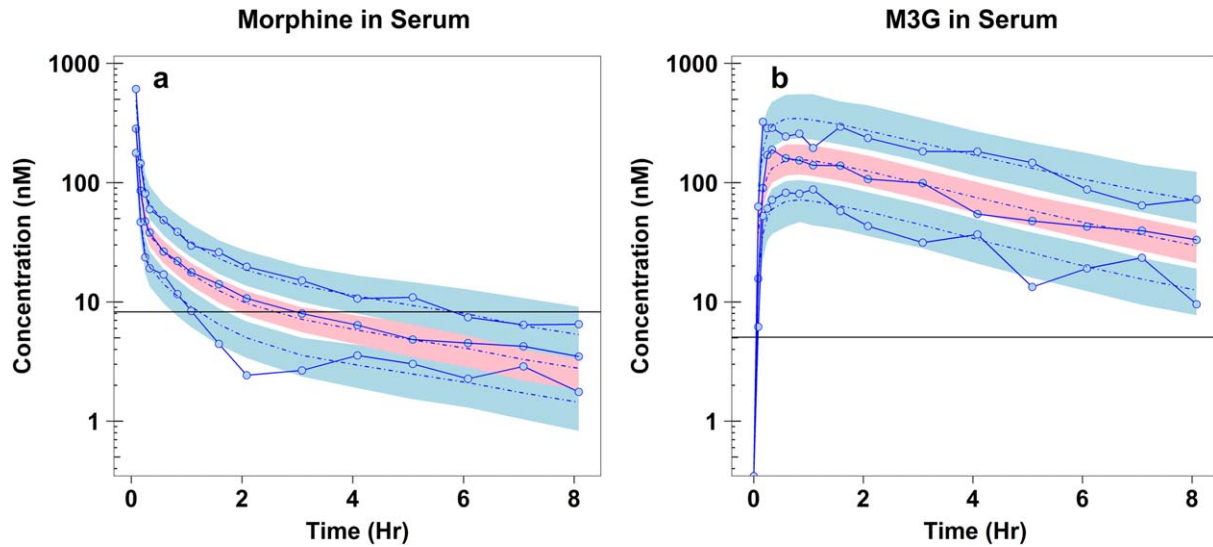
Figure 2 Final model visual predictive checks for (**a**) morphine and (**b**) morphine-3-glucuronide (M3G). Dotted and solid lines represent the 5th, 50th, and 95th percentiles of the simulated and observed data, respectively. Blue shaded areas represent the 95% prediction interval around the 95th and 5th percentile of the simulated data. Pink shaded areas represent the 95% prediction interval around the 50th percentile of the simulated data. The horizontal black lines represent the lower limit of quantification for morphine and M3G.

Population parameter estimates for the final model are shown in **Table 2.** All fixed effects parameters were estimated with acceptable precision (residual standard error <30%). Shrinkage estimates for random effect parameters were all <30%. A comparison of population parameter estimates to literature values for the final model using three separate methods of handling BLQ data are shown in **Supplementary Table S1**.

Visual inspection of final model diagnostic plots did not reveal any model misspecification (**Figure 2; Supplementary**

Figure S2-S4). Based on the results of the NPC, less than 10% of the observations fell outside of the 90% prediction interval for morphine and M3G model predictions in serum and urine, respectively (data not shown). The condition number for both the base and final model were below 1,000, which represents the conventional cutoff for model overparametrization and multicollinearity.[37] The NPDE plot for M3G was approximately normally distributed with deviations from normality for morphine due to the exclusion of BLQ observations when creating the NPDE plots (**Figure 3; Supplementary Figure S3,**

Table 2 Population parameter estimates for the final model

| Description	Parameter	Population estimate (RSE, %)	IIV, %CV (RSE, %)
Nonrenal clearance of morphine[a]	$CL_{M,NR}$ (L/hr)	44.1 (9)	31.6 (80)
Central volume of distribution of morphine[a]	V_M (L)	9.41 (13)	42.3 (55)
1st Peripheral volume of distribution of morphine[a]	VP1 (L)	108 (37)	—
1st Intercompartmental clearance of morphine[a]	QP1 (L/hr)	67.1 (17)	—
2nd Peripheral volume of distribution of morphine[a]	VP2 (L)	50.7 (21)	—
2nd Intercompartmental clearance of morphine[a]	QP2 (L/hr)	83.4 (15)	—
Renal clearance of morphine[a]	$CL_{M,R}$ (L/hr)	6.32 (11)	—
Total clearance of M3G	CL_{M3G} (L/hr)	7.32 (10)	34.5 (38)
Central volume of distribution of M3G	V_{M3G} (L)	9.51 (15)	56.6 (36)
Liver transit rate constant	k_{trans} (hr^{-1})	14.4 (14)	—
NASF effect on clearance of M3G[b]	NASF on CL_{M3G}	−0.628 (26)	—
Correlation between IIV CL_{M3G} and IIV V_{M3G}	Corr(CL_{M3G}-V_{M3G})	—	0.751 (20)
Residual variability (%)			
Proportional residual error of morphine in serum[c]	σ^2_M	27.2 (6)	—
Proportional residual error of M3G in serum[c]	σ^2_{M3G}	38.4 (10)	—
Proportional residual error of morphine in urine[c]	$\sigma^2_{M-Urine}$	62.1 (25)	—
Proportional residual error of M3G in urine[c]	$\sigma^2_{M3G-Urine}$	66.5 (22)	—

%CV, percent coefficient of variation; RSE, Relative standard error; IIV, inter-individual variability; M3G, morphine-3-glucuronide; CL, clearance; V, volume of distribution; Corr, correlation.

[a]Morphine volume and clearance parameters were allometrically scaled using total body weight.

[b]Fractional change in clearance of M3G for subjects with NASF scores above 4 using a natural logarithmic scale, where $CL_{M3G,i} = CL_{M3G,pop} * (1 - 0.6 * Ln(\frac{NASF_i}{4}))$ $* e^{(\eta_{CLM3G,i})}$ for the *i*th subject.

[c]Proportional residual error coded as additive on logarithmic scale.
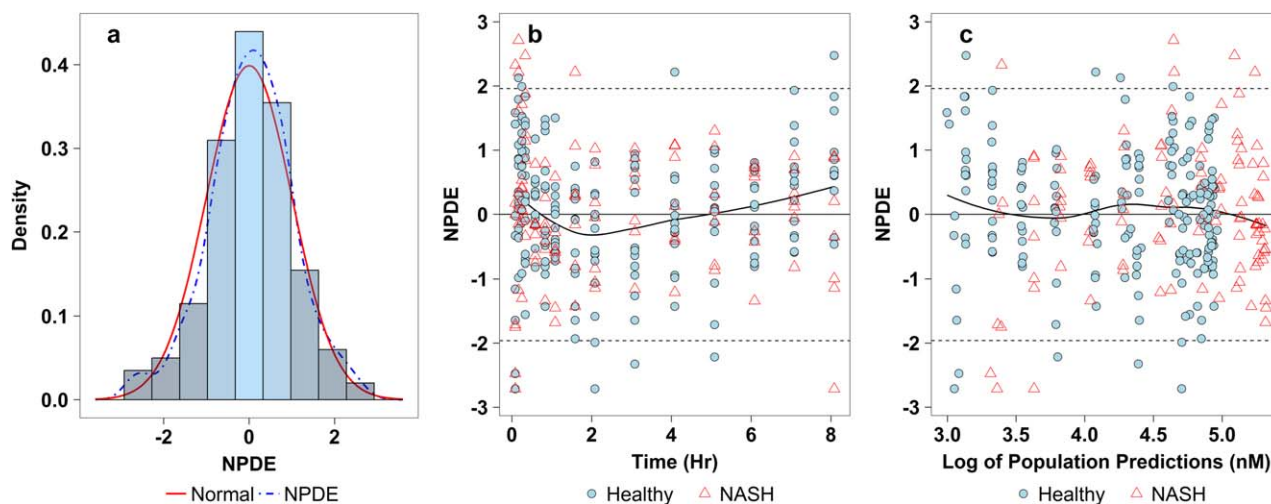
Figure 3 Normalized prediction distribution errors (NPDE) of morphine-3-glucuronide (M3G) in serum. (**a**) The dotted line represents the actual distribution of the NPDEs while the solid line reflects the normal distribution. (**b,c**) Red triangles and blue circles represent nonalcoholic steatohepatitis (NASH) and healthy subjects' NPDE values, respectively. The black line denotes the least squares fit for the combined data.

respectively). A VPC plot of the censored morphine observations showed acceptable model performance (**Supplementary Figure S4**). Individual *post-hoc* PK parameter estimates derived using the final model are shown in **Table 3**.

Simulations

Following a 10 mg (13.178 μmoles) morphine dose infused over 10 min every 4 h, the median (2.5th, 97.5th percentile) simulated serum $AUC_{M3G,SS,0-\tau}$ was significantly higher in virtual NASH subjects compared to virtual healthy subjects (2.03 μM*hr (1.00–4.03) vs. 1.28 μM*hr (0.641–2.55), $P < 0.0001$) (Figure 4). In contrast, the cumulative amount

excreted in urine over 4 hr for M3G after a single dose was similar for both groups (median (2.5th, 97.5th percentile) 6.48 μmoles (4.31–7.95) for healthy subjects vs. 6.73 μmoles [4.81–8.32] for NASH subjects, $P = 0.2$).

DISCUSSION

In a recent clinical study, morphine glucuronide exposure was significantly higher in NASH vs. healthy subjects.[21] These differences were attributed to changes in hepatic basolateral efflux transporter expression. Using the data from this study, a PopPK analysis was performed to characterize further the importance of NASH on morphine and morphine glucuronide disposition. The population estimates for CL_{M3G} and V_{M3G} were similar to those reported in the literature.[19,28] Although there is considerable variability in the published population estimates for CL_M (48–110 L/hr), the estimate obtained from our study (49.6 L/hr) was comparable to another study in healthy and terminally ill adults (48 L/hr). CL_M estimates reported across studies may vary due to demographic characteristics and disease status.[21,29,39–41] For example, our study subjects were older, which may have contributed to the lower morphine systemic clearance compared to those in other previously published studies.[17,42]

To identify the factors affecting changes in morphine glucuronide disposition in NASH subjects, only M3G data were used. The stepwise covariate analysis indicated that NASF score was a statistically significant covariate. NASF scores reduced the IIV in CL_{M3G} by 11%, which accounted for 43% of the total IIV for this parameter. Although a previous report noted that NASH subjects have reduced renal function compared to healthy volunteers matched for age, gender, and BMI, CL_{M3G} was not correlated with creatinine clearance in our study subjects.[43] The present study controlled for age, gender, and renal function; thus, it is

**Table 3** Individual parameter and exposure estimates stratified by disease status

Parameters	Healthy ($N = 14$)	NASH ($N = 7$)
V_{M3G} (L)	12.1 (7.25-23.1)	13.4 (5.41-21.3)
V_M (L)	11.5 (7.18-23.5)	9.48 (8.21-10.15)
$CL_{M,R}$ (L/hr)[a]	7.38 (5.47-8.29)	8.41 (6.51-10.3)
$CL_{M,NR}$ (L/hr)[a]	53.1 (32.4-98.1)	63.4 (45.2-85.4)
CL_{M3G} (L/hr)	8.43 (5.48 −16.3)	5.15 (4.21-10.54)
$AUC_{M,0-\infty}$ (μM*hr)[b]	0.125 (0.0671-0.206)	0.104 (0.781-0.148)
$AUC_{M3G,0-\infty}$ (μM*hr)[b]	0.713 (0.365-1.11)	1.20 (0.578-1.54)

Values are expressed as median (range).

NASH, nonalcoholic steatohepatitis; M3G, morphine-3-glucuronide; V_{M3G}, central volume of distribution of M3G; V_M, central volume of distribution of morphine; $CL_{M,R}$, renal clearance of morphine; $CL_{M,NR}$, non-renal clearance of morphine; CL_{M3G}, systemic clearance of M3G; AUC_M, area under the concentration time curve of morphine in serum; AUC_{M3G}, area under the concentration time curve of M3G in serum.

[a]CL_M (total systemic clearance of morphine)= $CL_{M,R}$ (renal clearance of morphine) + $CL_{M,NR}$ (non-renal clearance of morphine).

[b]Single dose area under the concentration versus time curve for morphine ($AUC_{M,0-\infty}$) and M3G ($AUC_{M3G,0-\infty}$) were estimated using model-derived parameters and according to the following equations: $AUC_{M,0-\infty} = \left(\frac{DOSE}{CL_M}\right)$ $AUC_{M3G,0-\infty} = \left(\frac{f_{M3G} * CL_M}{CL_{M3G}}\right) * AUC_{M,0-\infty}$ where the fraction of the morphine dose metabolized to M3G was assumed to be 1.
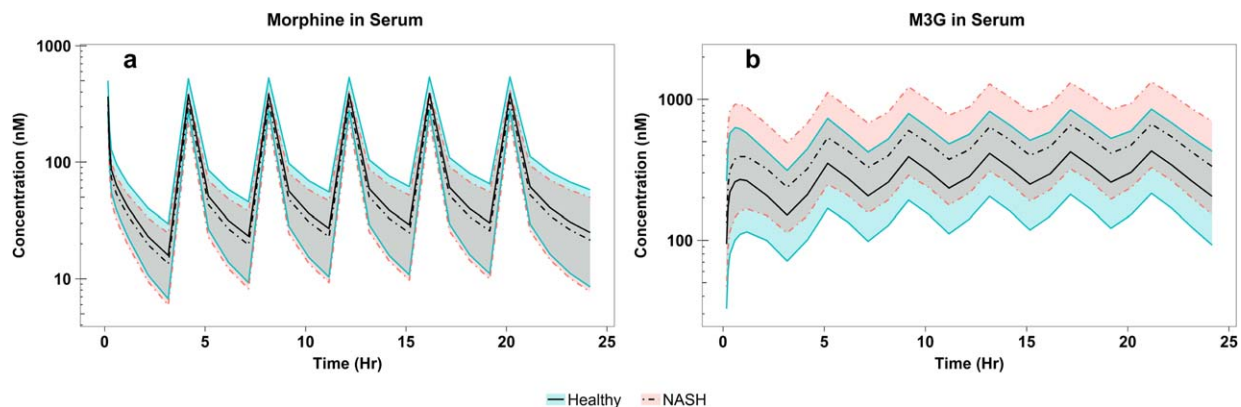
Figure 4 Simulated exposure of (**a**) morphine and (**b**) morphine-3-glucuronide (M3G) in serum over 24 hr following multiple doses of morphine 10 mg administered intravenously every 4 hr. Pink and blue shaded regions represent the 95% prediction intervals for non-alcoholic steatohepatitis (NASH) and healthy subjects, respectively. Dotted and solid lines represent 5th, 50th, and 95th percentiles for NASH and healthy subjects, respectively.

reasonable that creatinine clearance was not a significant covariate in this analysis. Also, since the systemic exposure of M3G has been shown to be insensitive to probenecid, alteration in renal transporter kinetics is unlikely to contribute to the observed reduction in CL_{M3G} for NASH subjects in this study.[11,44,45]

On the other hand, the biliary excretion of M3G was reported to be reduced by 48% in NASH-induced rats (resulting in a 1.5-fold increase in systemic exposure).[11] Biliary excretion of liver-formed M3G via apical (canalicular) Mrp2 can account for up to 30% of the administered morphine dose in mice. In fact, Mrp2-deficient mice exhibited a substantially reduced biliary excretion of M3G without a significant increase in the 24-hr urinary recovery of M3G despite the observed higher systemic exposure.[20] The reduced CL_{M3G} in the present model may reflect the combined effects of reduced biliary excretion and increased basolateral efflux of M3G, which would diminish intrahepatic and conversely increase systemic M3G exposure in NASH patients.

As developed, our model cannot characterize the nonrenal elimination of M3G and other routes of morphine metabolism independent of glucuronidation to M3G. Alternative elimination routes of morphine other than glucuronidation (e.g., renal elimination and N-demethylation) can account for over 20% of morphine clearance.[36] Hence, we cannot disregard the possibility that changes in morphine metabolism, including glucuronidation activity, and biliary excretion of liver-formed morphine glucuronides may, at least in part, explain the observed differences in M3G systemic disposition between NASH and healthy subjects in our study. Nonetheless, we would expect that increases in hepatic glucuronidation of morphine in NASH patients would be reflected by an increase in the systemic clearance of morphine along with a significantly higher urinary excretion of the glucuronide metabolites. Furthermore, as previously noted, the mRNA expression of UGT2B7 (enzyme responsible for conjugation of morphine) was not significantly different in human liver samples of NASH patients (fatty and nonfatty), patients with steatosis, and normal

subjects.[15] Thus, given the preclinical evidence for reduced biliary Mrp2 function in NASH rodents, and the similarity between the systemic morphine exposure and urinary excretion of morphine and its conjugated glucuronides between the NASH and healthy subjects in the present study, changes in M3G formation are less likely to explain our study findings.[12,15,21]

Alternatively, it is plausible that the observed differences in exposure and model-derived CL_{M3G} are transient effects that would eventually diminish over a longer sampling period. Since recent evidence suggests that the basolateral efflux rate of M3G is increased for NASH, there may be a higher initial amount of M3G that reaches the systemic circulation in patients with NASH, which leads to an increased area under the concentration vs. time curve for M3G during the observed 8-hr sampling interval.[6,11,46] Additional *in vivo* clinical studies are warranted to investigate these hypotheses and the clinical implications of these changes.

To assess the potential effects of NASH on the steady-state exposure of M3G, a multiple-dose simulation was performed. The simulation results illustrated that the steady-state M3G serum exposure was increased in NASH subjects, yet no significant difference was detected from the simulated 4-hr urinary M3G recovery data after a single 10-mg morphine dose. It is plausible that differences in the simulated urine M3G data were not detected due to the high residual variability for both morphine and M3G urine observations in the original dataset, which informs the model parameters for the simulation. In addition, it is also likely that the 4-hr collection window over which an average of 50% of the administered dose was excreted in urine was not sufficient to capture any differences between the simulated healthy and NASH subjects. These results further highlight the effect that NASH status and NASF severity scores may have on transporter substrates that exhibit hepatic and renal elimination pathways similar to the glucuronide conjugates of morphine.

Our analyses are not without limitations. Although PK sampling data were available, there were only seven NASH subjects, none of whom had detectable morphine

observations beyond 6 h. Thus, the small sample of NASH subjects in this study may have hindered the detection of other physiologically plausible covariates beyond NASF. The high variability in the M3G urine data restricted our ability to obtain reliable estimates of fraction metabolized to M3G. However, the same covariate model was obtained when the M3G urine data were ignored (data not shown). Although M6G is a more potent analgesic than its parent compound, this metabolite was not included in the analysis due to the high percentage of BLQ observations (42%). Nonetheless, there is limited evidence suggesting any differences in the systemic disposition of M3G and M6G. Thus, alterations in the serum disposition of M3G, the more prevalent metabolite, provide a more sensitive endpoint for this analysis compared to M6G.

In conclusion, changes in transporter kinetics in NASH subjects may contribute to altered disposition of drugs and metabolites that are substrates for these transporters, which could alter the efficacy or toxicity of compounds used to treat this population. This model effectively captured and quantified the difference in exposure between patients with NASH and healthy subjects for M3G. Therapeutic agents used in the management of hypercholesterolemia in NASH patients, such as rosuvastatin and ezetimibe, are known MRP3 and/or MRP4 substrates.[6,47] *In vivo* clinical studies are needed to explore further the implications of altered transporter kinetics on treatment efficacy or toxicity of highly transported drugs in patients with NASH.

Author Contributions. V.P. and D.G. wrote the article; V.P., C.K.J., B.C.F., K.L.B., and D.G. designed the research; V.P., C.K.J., B.C.F., K.L.B., and D.G. performed the research; V.P. analyzed the data.

Conflict of Interest. The authors declare no conflicts of interest.

1. Targher, G. & Byrne, C.D. Clinical review: nonalcoholic fatty liver disease: a novel cardiometabolic risk factor for type 2 diabetes and its complications. *J. Clin. Endocrinol. Metab.* **98**, 483–495 (2013).

2. Byrne, C.D. & Targher, G. NAFLD: a multisystem disease. *J. Hepatol.* **62**, S47–S64 (2015).

3. Vernon, G., Baranova, A. & Younossi, Z.M. Systematic review: the epidemiology and natural history of non-alcoholic fatty liver disease and non-alcoholic steatohepatitis in adults. *Aliment. Pharmacol. Ther.* **34**, 274–285 (2011).

4. Yu, J., Shen, J., Sun, T.T., Zhang, X. & Wong, N. Obesity, insulin resistance, NASH and hepatocellular carcinoma. *Semin. Cancer Biol.* **23**, 483–491 (2013).

5. Dietrich, P. & Hellerbrand, C. Non-alcoholic fatty liver disease, obesity and the metabolic syndrome. *Best Pract. Res. Clin. Gastroenterol.* **28**, 637–653 (2014).

6. Hardwick, R.N., Fisher, C.D., Street, S.M., Canet, M.J. & Cherrington, N.J. Molecular mechanism of altered ezetimibe disposition in nonalcoholic steatohepatitis. *Drug Metab. Dispos.* **40**, 450–460 (2012).

7. Clarke, J.D. & Cherrington, N.J. Nonalcoholic steatohepatitis in precision medicine: unraveling the factors that contribute to individual variability. *Pharmacol. Ther.* **151**, 99–106 (2015).

8. Merrell, M.D. & Cherrington, N.J. Drug metabolism alterations in nonalcoholic fatty liver disease. *Drug Metab. Rev.* **43**, 317–334 (2011).

9. Lake, A.D. *et al.* Analysis of global absorption, distribution, metabolism, and elimination gene expression in the progressive stages of human nonalcoholic fatty liver disease. *Drug Metab. Dispos.* **39**, 1954–1960 (2011).

10. Canet, M.J. *et al.* Modeling human nonalcoholic steatohepatitis-associated changes in drug transporter expression using experimental rodent models. *Drug Metab. Dispos.* **42**, 586–595 (2014).

11. Dzierlenga, A.L. *et al.* Mechanistic basis of altered morphine disposition in nonalcoholic steatohepatitis. *J. Pharmacol. Exp. Ther.* **352**, 462–470 (2014).

12. Hardwick, R.N., Fisher, C.D., Canet, M.J., Scheffer, G.L. & Cherrington, N.J. Variations in ATP-binding cassette transporter regulation during the progression of human nonalcoholic fatty liver disease. *Drug Metab. Dispos.* **39**, 2395–2402 (2011).

13. Canet, M.J. *et al.* Renal xenobiotic transporter expression is altered in multiple experimental models of nonalcoholic steatohepatitis. *Drug Metab. Dispos.* **43**, 266–272 (2015).

14. Hardwick, R.N., Fisher, C.D., Canet, M.J., Lake, A.D. & Cherrington, N.J. Diversity in antioxidant response enzymes in progressive stages of human nonalcoholic fatty liver disease. *Drug Metab. Dispos.* **38**, 2293–2301 (2010).

15. Hardwick, R.N. *et al.* Altered UDP-glucuronosyltransferase and sulfotransferase expression and function during progressive stages of human nonalcoholic fatty liver disease. *Drug Metab. Dispos.* **41**, 554–561 (2013).

16. Fisher, C.D. *et al.* Hepatic cytochrome P450 enzyme alterations in humans with progressive stages of nonalcoholic fatty liver disease. *Drug Metab. Dispos.* **37**, 2087–2094 (2009).

17. Villesen, H.H. *et al.* Pharmacokinetics of morphine and oxycodone following intravenous administration in elderly patients. *Ther. Clin. Risk Manag.* **3**, 961–967 (2007).

18. Joppich, R. *et al.* Analgesic efficacy and tolerability of intravenous morphine vs. combined intravenous morphine and oxycodone in a 2-center, randomized, double-blind, pilot trial of patients with moderate to severe pain after total hip replacement. *Clin. Ther.* **34**, 1751–1760 (2012).

19. Coffman, B.L., Rios, G.R., King, C.D. & Tephly, T.R. Human UGT2B7 catalyzes morphine glucuronidation. *Drug Metab. Dispos.* **25**, 1–4 (1997).

20. van de Wetering, K. *et al.* Multidrug resistance proteins 2 and 3 provide alternative routes for hepatic excretion of morphine-glucuronides. *Mol. Pharmacol.* **72**, 387–394 (2007).

21. Ferslew, B. *et al.* Altered morphine glucuronide and bile acid disposition in patients with nonalcoholic steatohepatitis. *Clin. Pharmacol. Ther.* **97**, 419–427 (2015).

22. Ferslew, B.C. *et al.* Altered bile acid metabolome in patients with nonalcoholic steatohepatitis. *Dig. Dis. Sci.* **60**, 3318–3328 (2015).

23. Keizer, R.J., van Benten, M., Beijnen, J.H., Schellens, J.H.M. & Huitema, A.D.R. Piraña and PCluster: a modeling environment and cluster infrastructure for NONMEM. *Comput. Methods Programs Biomed.* **101**, 72–79 (2011).

24. Lindbom, L., Pihlgren, P., Jonsson, E.N. & Jonsson, N. PsN-Toolkit–a collection of computer intensive statistical methods for non-linear mixed effect modeling using NONMEM. *Comput. Methods Programs Biomed.* **79**, 241–257 (2005).

25. R Development Core Team. R: a language and for statistical computing. R Foundation for Statistical Computing, Vienna, Austria. <https://www.r-project.org>

26. Karlsson, M. & Holford, N. A tutorial on visual predictive checks. *Abstracts of the Annual Meeting of the Population Approach Group in Europe.* <http://www.page-meeting.org/?abstract=1434> (2008).

27. Comets, E., Brendel, K. & Mentré, F. Computing normalised prediction distribution errors to evaluate nonlinear mixed-effect models: the npde add-on package for R. *Comput. Methods Programs Biomed.* **90**, 154–166 (2008).

28. Ahn, J.E., Karlsson, M.O., Dunne, A. & Ludden, T.M. Likelihood based approaches to handling data below the quantification limit using NONMEM VI. *J. Pharmacokinet. Pharmacodyn.* **35**, 401–421 (2008).

29. Lötsch, J., Skarke, C., Schmidt, H., Liefhold, J. & Geisslinger, G. Pharmacokinetic modeling to predict morphine and morphine-6-glucuronide plasma concentrations in healthy young volunteers. *Clin. Pharmacol. Ther.* **72**, 151–162 (2002).

30. Mould, D.R. & Upton, R.N. Basic concepts in population modeling, simulation, and model-based drug development-part 2: introduction to pharmacokinetic modeling methods. *CPT Pharmacometrics Syst. Pharmacol.* **2**, e38 (2013).

31. Santiago-Rolón, A., Purcell, D., Rosado, K. & Toro, D.H. A comparison of Brunt's criteria, the non-alcoholic fatty liver disease activity score (NAS), and a proposed NAS scoring that includes fibrosis in non-alcoholic fatty liver disease staging. *Proc. R. Health Sci. J.* **34**, 189–194 (2015).

32. Bondini, S., Kleiner, D.E., Goodman, Z.D., Gramlich, T. & Younossi, Z.M. Pathologic assessment of non-alcoholic fatty liver disease. *Clin. Liver Dis.* **11**, 17–23, vii (2007).

33. Lake, A.D. *et al.* Decreased hepatotoxic bile acid composition and altered synthesis in progressive human nonalcoholic fatty liver disease. *Toxicol. Appl. Pharmacol.* **268**, 132–140 (2013).

34. Angulo, P. *et al.* The NAFLD fibrosis score: a noninvasive system that identifies liver fibrosis in patients with NAFLD. *Hepatology* **45**, 846–854 (2007).

35. Acharya, C., Hooker, A.C., Türkyýlmaz, G.Y., Jönsson, S. & Karlsson, M.O. A diagnostic tool for population models using non-compartmental analysis: the ncappc package for R. *Comput. Methods Programs Biomed.* **127**, 83–93 (2016).

36. Hasselström, J. & Säwe, J. Morphine pharmacokinetics and metabolism in humans. Enterohepatic cycling and relative contribution of metabolites to active opioid concentrations. *Clin. Pharmacokinet.* **24**, 344–354 (1993).

37. Uslu, V.R., Egrioglu, E. & Bas, E. Finding optimal value for the shrinkage parameter in ridge regression via particle swarm optimization. *Am. J. Intell. Syst.* **4**, 142–147 (2014).

38. Meineke, I. *et al.* Pharmacokinetic modelling of morphine, morphine-3-glucuronide and morphine-6-glucuronide in plasma and cerebrospinal fluid of neurosurgical patients after short-term infusion of morphine. *Br. J. Clin. Pharmacol.* **54**, 592–603 (2002).

39. Sverrisdóttir, E. *et al.* A review of morphine and morphine-6-glucuronide's pharmacokinetic-pharmacodynamic relationships in experimental and clinical pain. *Eur. J. Pharm. Sci.* **74**, 45–62 (2015).

40. Bouwmeester, N.J., Anderson, B.J., Tibboel, D. & Holford, N.H.G. Developmental pharmacokinetics of morphine and its metabolites in neonates, infants and young children. *Br. J. Anaesth.* **92**, 208–217 (2004).

41. Romberg, R. *et al.* Pharmacokinetic-pharmacodynamic modeling of morphine-6-glucuronide-induced analgesia in healthy volunteers: absence of sex differences. *Anesthesiology* **100**, 120–133 (2004).

42. Baillie, S.P., Bateman, D.N., Coates, P.E. & Woodhouse, K.W. Age and the pharmacokinetics of morphine. *Age Ageing* **18**, 258–262 (1989).

43. Targher, G. *et al.* Relationship between kidney function and liver histology in subjects with nonalcoholic steatohepatitis. *Clin. J. Am. Soc. Nephrol.* **5**, 2166–2171 (2010).

44. Somogyi, A.A. *et al.* Plasma concentrations and renal clearance of morphine, morphine-3-glucuronide and morphine-6-glucuronide in cancer patients receiving morphine. *Clin. Pharmacokinet.* **24**, 413–420 (1993).

45. Xie, R., Bouw, M.R. & Hammarlund-Udenaes, M. Modelling of the blood-brain barrier transport of morphine-3-glucuronide studied using microdialysis in the rat: involvement of probenecid-sensitive transport. *Br. J. Pharmacol.* **131**, 1784–1792 (2000).

46. Clarke, J.D., Hardwick, R.N., Lake, A.D., Canet, M.J. & Cherrington, N.J. Experimental nonalcoholic steatohepatitis increases exposure to simvastatin hydroxy acid by decreasing hepatic organic anion transporting polypeptide expression. *J. Pharmacol. Exp. Ther.* **348**, 452–458 (2014).

47. Pfeifer, N.D., Yang, K. & Brouwer, K.L.R. Hepatic basolateral efflux contributes significantly to rosuvastatin disposition I: characterization of basolateral versus biliary clearance using a novel protocol in sandwich-cultured hepatocytes. *J. Pharmacol. Exp. Ther.* **347**, 727–736 (2013).

Supplementary information accompanies this paper on the *CPT: Pharmacometrics & Systems Pharmacology* website (http://psp-journal.com)